Volume 10 | Number 33 | 7 September 2018 | Pages 4009–4106

Analytical Methods

rsc.li/methods

ISSN 1759-9679

ROYAL SOCIETY OF CHEMISTRY

PAPER
Carlos D. Garcia *et al.*
Carbon tape as a convenient electrode material for electrochemical paper-based microfluidic devices (ePADs)

Analytical Methods

PAPER

View Article Online
View Journal | View Issue

Cite this: *Anal. Methods*, 2018, **10**, 4020

Carbon tape as a convenient electrode material for electrochemical paper-based microfluidic devices (ePADs)†

Federico J. V. Gomez,‡[a] Paige A. Reed,‡[b] Diego Gonzalez Casamachin,[c] Javier Rivera de la Rosa,[c] George Chumanov,[b] Maria Fernanda Silva[a] and Carlos D. Garcia*[b]

Electrochemical paper-based analytical devices represent an innovative and versatile platform for fluid handling and analysis. Nevertheless, the intrinsic structure of the paper can impose limitations to both the selection of the electrode material and the method selected to attach the electrodes to the device, potentially affecting the analytical performance of the device. To address these limitations, we herein propose carbon tape as a simple and low cost alternative to develop ePADs. The proposed material (in the form of tape or tabs) was first characterized using a combination of contact angle analysis, resistivity, Raman spectroscopy, cyclic voltammetry, and electrochemical impedance spectroscopy. Upon this initial assessment, carbon tape was selected and modified with carbon nanotubes, to provide not only a better surface for proteins to adhere to, but also an enhanced electroactive surface. The analytical performance of the resulting device was assessed by integrating three enzymes that facilitate the oxidation of ethanol, glucose, and phenol, and by performing the detection of these analytes in beer samples. The resulting device, for which materials cost less than a dollar, represents a simple alternative material for ePADs, applied in this case to monitor three of the most important parameters during the production of beers.

Received 7th April 2018
Accepted 15th July 2018

DOI: 10.1039/c8ay00778k

rsc.li/methods

1. Introduction

Paper-based microfluidic devices (μPADs) represent an innovative platform for fluid handling and analysis.[1,2] Since their re-introduction in the late 2000s, these devices have been extensively used in diverse clinical, environmental, and defense applications.[3–6] The advantages of this technology over traditional microfluidic platforms include lower cost, simplicity, portability, and versatility.[7–9] A variety of detection methods have been integrated to μPADs including, but not limited to, colorimetry, fluorescence, and luminescence.[1,10] Among these, the most common detection method is colorimetry which, despite its simplicity, features a performance that is often limited by a narrow dynamic range, low sensitivity, and variability due to environmental illumination.[11,12] To overcome these limitations, electrochemical paper-based analytical devices (ePADs) were introduced by Dungchai *et al.*[12] Electrochemical detection improves upon simple colorimetric detection because of the inherent sensitivity, availability of low cost potentiostats, and the potential to be integrated with portable platforms.[6–9,13–15] Furthermore, electrochemical detection allows the balancing of the sensitivity and selectivity of the analysis by virtue of the selection of both the electrode material and the operating potential.[12] Additionally, the intrinsic wicking properties of the paper can be used to deliver the analyte to the electrode surface and increase the accuracy of time-dependent measurements.[12] Because of these advantages over other detection methods, the development of electrochemical detection is considered one of the most promising alternatives for μPADs.

As reported for previous electrochemical detection modes, the electrode composition typically dominates electrochemical behavior and functionality,[13] making the material one of the most important factors in the development of analytical methods. The materials that are widely used for the production of working electrodes on ePADs are metal-based[16] and carbon-based inks, which are deposited *via* painting, screen-printing or stencil methods.[10] Although these electrodes offer adequate performance and reliability, the inks and pastes often used for their production suffer from high electrical resistance (due to the presence of polymer binders) and lead to non-uniform electrode surfaces, potentially compromising the applicability of the devices.[10,17] Besides penetrating into the paper substrate

[a]*Instituto de Biología Agrícola de Mendoza (IBAM-CONICET), Facultad de Ciencias Agrarias, Universidad Nacional de Cuyo, Mendoza, Argentina*

[b]*Department of Chemistry, Clemson University, 211 S. Palmetto Blvd., Clemson, SC 29634, USA. E-mail: cdgarci@clemson.edu*

[c]*Universidad Autónoma de Nuevo León, Facultad de Ciencias Químicas, San Nicolás de los Garza, Nuevo León, Mexico*

† Electronic supplementary information (ESI) available. See DOI: 10.1039/c8ay00778k

‡ Authors contributed equally to the presented work and share first authorship, written order was determined alphabetically by surname.

(decreasing the available area), these inks can be a significant fraction of the cost, as they range from $90 to $500 for 10 mL of carbon-based inks and around $400 for 25 g of silver-nanoparticles based inks.[18] Besides the material, both the flexibility of the material and the attachment of the electrodes to the paper still present challenging aspects and can potentially have an adverse effect on the electrode's performance.[1,12,19] Aiming to address some of these limitations, this report describes the potential advantages of two carbon-based materials (tabs and tape) as a simple alternative to develop ePADs. The selected materials are inexpensive ($15–$40 per package) and widely available, as they are usually used to provide electrical contacts for electron microscopy. Due to their flexibility and their adhesive properties, the materials enable straightforward attachment to the paper substrate as well as the attachment of electrical leads to the electrode. This simple method makes ePADS ready for use in minutes. Here, the characterization of these electrodes and their application toward the enzyme-mediated detection of ethanol, glucose, and phenols is described. The proposed ePADs were used to monitor the selected analytes in beer samples.

2. Materials and methods

2.1 Reagents

All aqueous solutions were prepared using 18 MΩ cm water (NANOpure Diamond, Barnstead; Dubuque, IA) and analytical-grade chemicals. Phosphate buffer solutions (PBS) were prepared by dissolving anhydrous Na_2HPO_4 (Fisher Scientific; Fair Lawn, NJ, USA) in ultrapure water. The pH of the solutions was measured using a combined glass electrode connected to a digital pH meter (Orion 420A+, Thermo; Waltham, MA, USA) and adjusted with 1 M solutions of either NaOH or HCl. Two conductive carbon materials were initially selected as potential electrodes: sheets of carbon tape (#16085-1) and carbon tabs (#16084-3), both from TedPella (Redding, CA). According to the manufacturer, the conductive adhesive is a carbon-filled acrylic, free of solvents, which may contain very small impurities of Al and Si. Both materials are commonly used in electron microscopy and exhibit promising electrical properties. For the modification of the electrodes, as-received multi-walled carbon nanotubes (CNT; Sigma-Aldrich; St. Louis, MO) were used.

2.2 Preparation of the paper-based microfluidic device

The paper-based devices were fabricated from 3MM Whatman™ Chromatography Paper and cut into a six-spoked wheel design (Fig. 1). The six spokes were chosen to allow for multiple electrodes and therefore perform multiple tests per device. The design allows great versatility, leaving one electrode area available for the background and five other areas for analyte detection. Furthermore, the electrode areas can be easily modified with a bio-recognition element, such as an enzyme, to provide specificity or a redox active byproduct to the device, or left unmodified for the detection of naturally redox active materials such as metals.

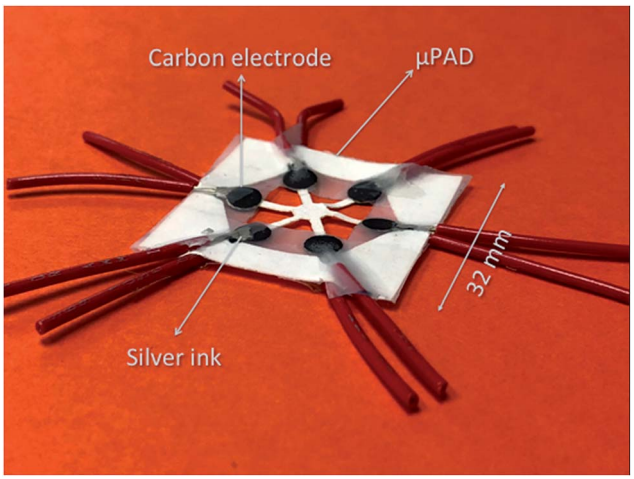

Fig. 1 Photograph of the paper-based microfluidic device with the electrical connections, shown against a colored background.

The μPAD was cut using an Epilog Mini Laser Engraver, equipped with a 30 W CO_2 laser. To minimize the possibility of igniting the devices (or damaging the edges of the device), a steady flow of nitrogen gas and 50% speed/50% laser power were utilized.[20,21] Unlike wax printing or photolithography,[22] the CO_2 laser not only defines the geometry of the device but also creates hydrophobic edges that help retain the solution within the device.[20] Each device was designed to fit within a square with a side length of 32 mm, yielding eight devices per sheet of paper. Each device was composed of six channels (length = 12.5 mm) and six circular electrodes (diameter = 4 mm).

2.3 Raman spectroscopy

Raman spectra were excited with a 514.5 nm light from an Ar^+ ion laser (Innova 200, Coherent, 500 mW). The scattered light was collected using a f/1.2 camera lens (Nikon) in a 45° back-scattering geometry and analyzed by using a triple spectrometer (Triplemate 1877, Spex) equipped with a CCD camera (iDUS 420, Andor). The spectral resolution at the excitation wavelength was 0.2 nm. Raman spectrum of indene was used for the spectral calibration.

2.4 Electrochemical techniques

To investigate the electrochemical performance of the two carbon materials, cyclic voltammetry (CV) and electrochemical impedance spectroscopy (EIS) were performed in 0.1 M phosphate buffer as supporting electrolyte with 0.1 M $Fe(CN)_6^{3-}$/$Fe(CN)_6^{4-}$ as the redox couple. A CHI660A Electrochemical Analyzer (CH Instruments, Inc.; Austin, TX) was used for these measurements. EIS data were obtained by scanning from 10^{-4} Hz to 10^5 Hz at a 5 mV amplitude, with 10 data points per frequency decade. The impedance spectra were then analyzed with the simulation software Zview-Impedance® (version 2.4a) by fitting the spectra with a Randles-type equivalent circuit. A standard three-electrode cell composed of the carbon tabs or tape, a commercial Ag|AgCl|KCl_{sat} electrode, and a platinum wire were used as the working, reference, and counter

electrodes, respectively. Stripped 22-gauge tinned copper wires and conductive silver ink (SPI supplies #05002-AB, West Chester, PA) were used to provide electrical contact. This connection was sealed using three coats of liquid electrical tape (Performix; Blaine, MN). It is critical to point out that the seal requires at least 4 hours to cure and experiments performed with partially cured seals yielded a number of experimental artifacts (data not shown).

2.5 Contact angle and resistivity

To gain preliminary information related to the macroscopic properties of the proposed carbon tape materials, both contact angle and resistivity were determined. The contact angle was studied to evaluate the wettability of the electrode by placing a drop (5 μL) of ultrapure water onto a bare carbon tape electrode and taking a lateral black and white picture of the droplet with a smart phone camera. The contact angle was then measured using the Low Bond Axismmetric Drop Shape Analysis (LB-ADSA) plugin for ImageJ software.[23] Resistivity measurements were obtained with a Keithley 2636A SourceMeter coupled to a Jandel cylindrical four-point probe (Leighton Buzzard, England) with a 1 mm probe spacing. The thickness of the material was then confirmed using scanning electron microscopy (SEM). The measured resistivity values were compared to those of other, well-known, carbon electrodes reported in the literature.

2.6 Electrochemical detection

For simplicity, the proposed ePAD was fabricated considering a standard two-electrode array. To improve the catalytic activity of the detection electrodes, CNTs were added to the paper (at the detection spot) by dispensing 5 μL of an ethanoic suspension containing 0.05 mg mL^{-1} CNTs (this suspension was placed in the ultrasonic bath for 30 min prior to use to disperse the CNTs). After allowing the ethanol to evaporate, the chips were rinsed with phosphate buffer to remove the loosely bound CNTs. Three different enzymes were then placed at three different electrode areas to allow for multi-analyte detection: 1 mg mL^{-1} alcohol oxidase was placed at electrode area #1, 1 mg mL^{-1} glucose oxidase was placed at electrode area #3, and 1 mg mL^{-1} tyrosinase was placed at electrode area #5. All three enzymes were deposited in the same way: 5 μL of sample was deposited on top of the dried CNTs and allowed to dry at room temperature for 30 min to ensure adsorption onto the paper substrate, as demonstrated in our previous work.[24] Carbon electrodes, cut into 4 mm diameter circles using the laser engraver, were placed over the CNT-modified μPAD. An identically shaped carbon tape electrode was also placed on the opposite side of the device, to serve as the counter/pseudo-reference electrode. Stripped 22-gauge tinned copper wires were then placed on both electrodes using the inherent adhesive properties of the tape. Conductive silver ink (SPI supplies #05002-AB, West Chester, PA) was then painted on both the tinned copper wires and the carbon tape electrodes to improve the electrical contact. The silver ink was allowed to cure at room temperature for 5 minutes before sealing, along the edge of the electrode, with scotch tape. A commercial transfer press was used to seal the tape into place (heating function was not turned on to preserve the activity of the enzymes).

2.7 Beer samples

To challenge the device with a complex sample, five beers and one cider were sampled for the alcohol, sugar, and total phenol content. Samples were purchased at a local liquor store and were stored at 4 °C to preserve the contents prior to measurements. For the analyses, aliquots were taken by pipetting 30 μL of each sample onto the center of the device and allowing 30 s for the sample to wick (Fig. 3). Afterwards, 3 measurements were taken for each enzyme area (15 s each) and a blank, resulting in an overall analysis time of 3 minutes for all analytes and a total analysis time of 3.5 minutes.

3. Results and discussion

3.1 Characterization of the carbon materials

As the first approach to characterize the two carbon materials (tape and tabs), resistivity (ρ) was determined according to eqn (1), where A represents the cross-sectional area and l is the distance between the two measuring electrodes. In both cases, the resistance (Ω) of the electrodes was measured using a 4-point probe and the material thickness was measured using SEM (260 ± 10 μm for the tape and 125 ± 7 μm for the tabs). These values are in agreement with those reported by the manufacturer.

$$\rho = \Omega A/l \quad (1)$$

While both materials exhibited low resistivity (in the order of mΩ cm), the carbon tape featured a slightly lower value than that for carbon tabs (Table 1). It is worth mentioning that the resistivity of both materials is significantly lower than the reported value for Bellpale C-2000 commercial glassy carbon electrodes[25] as well as other standard carbon-based electrodes.[26–29]

The wettability of the carbon materials was examined by measuring the contact angle between the surface and a water droplet at room temperature. As can be seen in Table 1, both carbon materials had contact angles <90°, suggesting that the materials are only partially hydrophilic. These values are

Table 1 Characterization of the two carbon materials by film resistivity, contact angle, EIS, and CV. Experimental conditions are as described in Fig. 2

	Carbon tape	Carbon tabs
Resistivity (mΩ cm)	1.0 ± 0.2	6 ± 1
Contact angle (°)	73 ± 1	57 ± 1
R_{sol} (Ω)	48 ± 1	48 ± 1
R_{film} (kΩ)	33 ± 9	37 ± 2
R_{ct} (kΩ)	80 ± 4	142 ± 5
C (μF)	7 ± 1	5.5 ± 0.6
CPE (μF)	201 ± 2	352 ± 6
α	0.839 ± 0.007	0.819 ± 0.007
ΔE_p at 100 mV s^{-1} (mV)	437.8 ± 0.8	453.6 ± 0.7

slightly larger than those of other carbon-based materials,[30–32] which (without the adhesive layer) display an average value of approximately 75°. It is also important to point out that the adhesive layer (~30 μm), which can be responsible for the slightly higher hydrophobic character of the surface, has not represented a significant problem for this application. Should such a layer impose any limitations to other applications, the adhesive can be removed using ethyl acetate, ethanol, or isopropanol.

To investigate the structure of the carbon material included in the electrodes, Raman spectra were collected.[33] The experiments focused on two relevant peaks, at 1360 cm^{-1} (disorder-induced D-band) and 1590 cm^{-1} (symmetry-allowed G-band of graphitic materials).[34] In agreement with previously reported approaches,[26] the D/G ratio was then calculated and compared to other materials to estimate the relative abundance of the disordered and graphitic fraction. As can be observed in Fig. 2A, clear Raman signals were obtained for both samples, yielding a D/G ratio of 0.86 and 1.16 for the carbon tabs and tape, respectively. These values not only correlate with the lower resistivity observed for the carbon tape but also are in line with other carbon-based materials used as working electrodes.[35]

In order to obtain information about the electrochemical activity of the carbon electrodes, cyclic voltammograms were recorded as a function of sweep rate. For these experiments, $Fe(CN)_6^{3-/4-}$ was selected as a model inner sphere electrochemical couple, likely to evidence adsorption (hydrophobic effects).[36] As can be observed in Fig. 2B, the peak current of both the reduction and oxidation electrochemical processes increased linearly with the square root of the scan rate for both carbon electrodes, suggesting that the rate of electron transfer was comparable to the mass transport rate (quasi-reversible behavior). In stark contrast to a fully reversible behavior, both electrodes yielded a ΔE_p that was highly dependent on the scan rate and that ranged from 200 mV to almost 500 mV for both materials (within the interval studied, Fig. 2C). These results are characteristic of slow electron transfer kinetics and indicate that the performance of electrodes could be limited by the electrical resistance of the material.[26] In addition, it is important to mention that voltammograms obtained with carbon tabs also showed additional peaks, suggesting the presence of additional electroactive species on the surface of the material (ESI†).

Electrochemical impedance spectroscopy (EIS) was carried out to obtain quantitative information about the electrical behavior of the carbon materials and rationalize the results

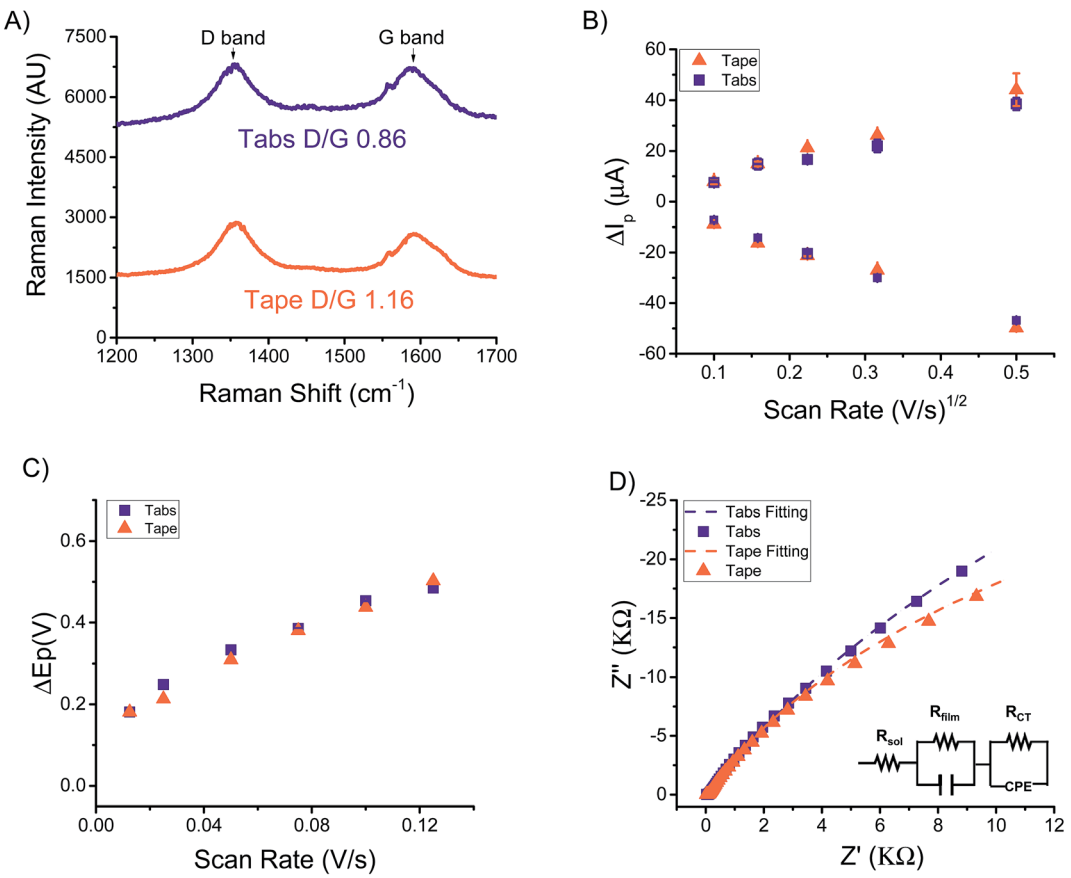

Fig. 2 (A) Raman spectrograph of the two carbon materials. (B) Dependence of the peak current ($\Delta I_p = I_{pFerri/Ferro} - I_{pBlank}$) on the sweep rate for both the reduction and oxidation processes on the two carbon materials. (C) Dependence of the peak potential difference on the sweep rate for both materials. (D) Experimental (symbols) and model-generated (lines) Nyquist plots obtained for the two carbon materials. Figures (B–D) were obtained with 0.1 M phosphate buffer as the supporting electrolyte and 0.1 M $K_3Fe(CN)_6$ as the redox couple.

obtained by CV. 0.1 M $Fe(CN)_6^{3-/4-}$ was also used as the redox couple and the potential applied (+600 mV) was selected from the voltammograms to maximize the current. The obtained spectra was then fitted with a Randles-type equivalent electrical circuit (see insert in Fig. 2D), containing elements representing the resistance of the solution (R_{sol}), the internal resistance of the film (R_{film}), the charge transfer resistance (R_{ct}), the capacitance of the film (C), and surface capacitance (CPE). To account for the heterogeneity and roughness of the electrodes, the capacitance of the surface was modelled with a constant phase element (CPE, $\alpha = 0.839$ and 0.819 for the tape and tabs, respectively) instead of a traditional capacitor.[37–39] Table 1 presents a summary of the fitting results, which are within the range reported for other carbon electrodes[27,28,40] and suggest that the electrochemical process is limited by the charge transfer resistance.[26]

Overall, these results indicate that the carbon tabs and the carbon tape are similar products, with similar composition, contact angle, resistivity, and electrochemical properties. The main difference between the two materials was the peak shape of the cyclic voltammograms; the tape demonstrated clear, distinct peaks while the carbon tabs provided voltammograms with less defined signals (ESI†). In addition, the charge transfer resistance was also found to be slightly lower for the carbon tape (80 kΩ *vs.* 142 kΩ). While technically either material could be used to develop ePADs, we have also considered the overall cost: the cost for carbon tabs was three times as high as that for the carbon tape ($0.074 per electrode *vs.* $0.027 per electrode). With this cost efficiency in mind as well as considering the lower resistivity and higher charge transfer, carbon tape was chosen as the carbon material for the ePAD and was used in all subsequent experiments.

3.2 Design of the paper based microfluidic device

A six-spoked wheel design was chosen to allow for multiple electrodes and thus multiple analytes per chip, increasing the throughput of the approach. In order to define the sample volume required to wick the device, increasing amounts of buffer were spotted onto the center of the chip. Next, photographs of the chips were taken at 10 s intervals for 60 s using a smartphone camera, to analyze the distance the solution travelled. To analyze the photos, CorelDraw software was used. As can be observed in Fig. 3, a minimum of 30 μL was required to ensure that the sample reached the detection spots, therefore defining the minimum sample volume. It is also important to point out that it only required 30 s for the solution (30 μL) to wick the chip, adding to the advantages of the platform.

3.3 Tailoring the device towards the detection of H_2O_2

One of the potential advantages of the proposed electrodes is that they could be integrated into a variety of electrochemical methodologies, including the development of biosensors. Therefore, CNTs were added to the device not only to improve the electrochemical activity of the electrodes[41] but also to provide a convenient support to immobilize enzymes.[42–44] Rather than modifying the electrode's surface with the CNT,

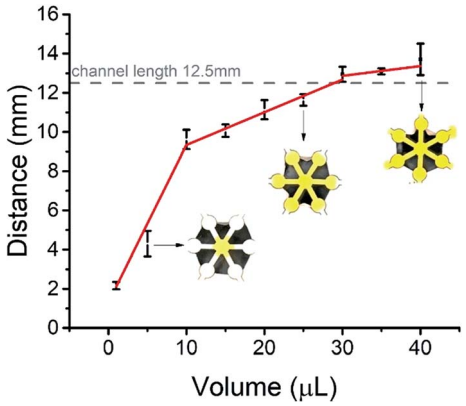

Fig. 3 Effect of sample volume on the distance travelled by the colored water. Photographs shown on the figure are 30 s after the colored drop of water was placed in the center of the microfluidic device.

which would have negatively affected the adhesive properties of the surface, the CNTs were deposited on the paper substrate. The electrochemical response from 10 mM H_2O_2 (also prepared in PBS) was measured in order to determine the optimum amount of CNTs required. As can be observed in Fig. 4A, only a marginal signal was observed when the devices without CNTs were tested. This observation is consistent with previous literature reports describing the poor performance of plain carbon electrodes towards the electrochemical detection of peroxide.[45] Upon the addition of CNTs, progressively increasing amperometric signals were measured with the addition of CNTs until an apparent plateau was reached at 25 ng (5 μL of the suspension containing 0.05 mg mL^{-1}). Further increase of the CNTs (up to 50 ng) only resulted in slight increases in the electrochemical response. These results demonstrate that despite not being directly deposited onto the electrode, the CNTs nevertheless are electrically connected to the carbon tape, providing significant improvement of the electrochemical response when compared to the carbon tape without CNTs. 25 ng of CNTs was

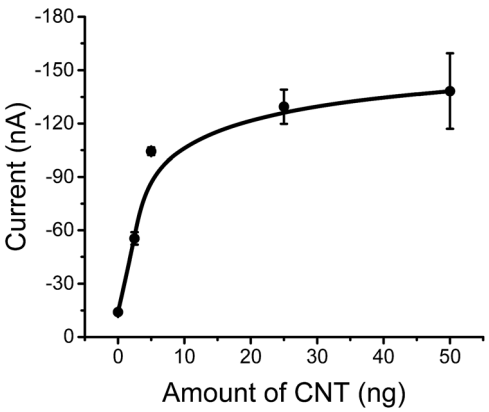

Fig. 4 Dependence of the anodic current as a function of the amount of CNTs applied to the device. Conditions: detection potential = −50 mV, 10 mM H_2O_2 in 0.1 M phosphate buffer as the supporting electrolyte.

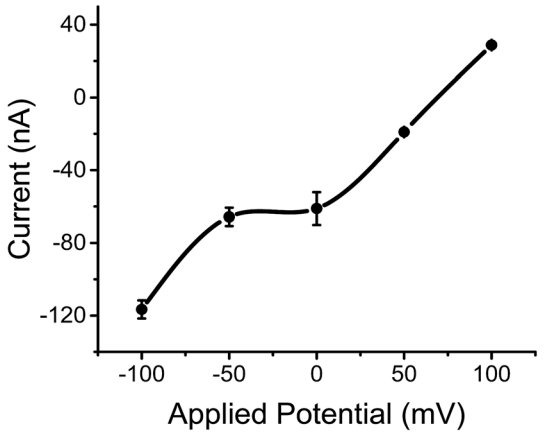

Fig. 5 Hydrodynamic voltammogram of 10 μM H_2O_2 using 0.1 M phosphate buffer as the supporting electrolyte.

deemed to be the optimal compromise between the amount of CNTs used and the intensity of the electrochemical signal. This amount of CNTs was used in all relevant experiments. Although individual CNTs cannot be directly observed by SEM, which reveals only the morphology of the cellulose substrate, the presence of CNTs on the surface of the fibers was confirmed by EDS (see ESI†).

The optimal applied potential for the amperometric detection was determined by performing a pseudo-hydrodynamic voltammogram. In this case, a solution containing 0.01 mM H_2O_2 was dispensed in the center spot and allowed to wick across the device. Then, detection potentials ranging from −100 mV to +100 mV were applied to each electrode, to generate the typical *i*–*t* profiles. Following previous reports,[12] the potential limits were selected to avoid extraneous redox processes and provide selectivity to the detection step. In all cases, the current intensity at 5 s (time when a steady current was observed) was recorded and plotted against the applied potential. It can be observed in Fig. 5 that there was a significant increase in the current as the potential decreased from +100 mV to −100 mV. When potentials within the 0 mV to −50 mV range were applied, relatively stable current signals were obtained for the reduction of H_2O_2. Based on this response, which is typical of carbon electrodes,[12] −50 mV was selected as an optimum potential for the reduction of hydrogen peroxide and used to investigate the sensitivity of the ePADs.

Under the optimum conditions, a linear relationship between the current and the concentration of H_2O_2 was obtained in the 100 nM to 100 mM concentration range (I_p, nA = 0.69 ln[H_2O_2, M] + 13.83; R^2 = 0.9993). While this dynamic range is a clear advantage over previous devices,[22,46] it is important to acknowledge that the sensitivity of the system should be further improved (slope in the semi-log scale).

Also using the optimum conditions for the detection of H_2O_2, the reproducibility of the fabrication procedure was evaluated. In this case, the results obtained with different devices (n = 6) were found to be within a 7% range, which was considered acceptable for the scope of the project.

3.4 Analysis of beer samples

The brewing process can be considered one of the oldest forms of biotechnology. Today's overall market for beer is $110 billion, with much of the market's gains attributed to craft beers ($26 billion, 8% annual growth).[47] However the success, safety and taste of beers depend on an intricate balance of the selected water, yeast, sugars (malt, barley, *etc.*), and flavoring agents (hops).[48–50] In some cases, fruits, herbs, or spices can be also added to give beer a particular taste.

As a result, these ingredients result in a complex sample that presents a challenge for analytical chemistry.[51–54] Among pH and other important analytes (including free amino acids, SO_2, proteins, and biogenic amines),[55] the final content of carbohydrates, alcohol, and phenolic compounds are of tremendous importance. Carbohydrates not only support the fermentation process but also contribute to the taste (sweetness), body, and caloric content of the beer.[48] Among the fermentable sugars present in beer (fructose, glucose, maltose, and maltotriose),[56] glucose is one of the most abundant components and is of critical importance. The alcohol content (referring to the ethanol content) not only is an important asset for the beer in terms of calories and alcohol intake by the customer,[50] but also represents an important marker to monitor the fermentation process. Last but not the least, phenolic compounds contribute to the colloidal stability, antioxidant capacity, and shelf life of beer. Along with alpha acids and a few other compounds, phenolic compounds contribute to the distinct bitter taste of some beers.[49] To analyze carbohydrates, alcohol, and phenolic compounds in beer using the proposed ePAD, three oxidases where incorporated: glucose oxidase, alcohol oxidase, and tyrosinase. While the first two enzymes result in the formation of H_2O_2, tyrosinase catalyzes the oxidation of phenols to the corresponding quinones. Besides providing selectivity towards the selected analytes, these enzymes also represent a simple way to benchmark the performance of our device against previous literature reports. It is also important to point out that due to the difference in the reaction mechanism, a separate hydrodynamic experiment was performed using 0.01 mM phenol as a model compound. In this case, the optimal potential for the reduction of benzo-quinone (the product of phenol with tyrosinase) was also found to be −50 mV (see ESI†). In order to determine the suitability of our device to provide useful information related to the production of beer,[57–61] these optimum analytical conditions were applied to investigate the response of the device towards the three selected analytes. The results are summarized in Table 2, where the calculated limit of detection (LOD, 3 × SD_{blank}/slope), linear range, and sensitivity are included. As can be noticed, the proposed strategy yields limits of detection similar to those recently reviewed[11,13] and reported for alcohol,[62] glucose,[12] and phenolic compounds.[4,63]

Five beers and one cider were analyzed for their glucose, ethanol, and phenol concentration using the proposed ePAD. As summarized in Table 3, good agreements between the measured concentrations and the concentrations declared by the manufacturers were obtained. It is important to mention that although the sugar content of the cider was reported to be

Table 2 Figures of merit for the selected analytes with 10 mM phosphate buffer as the supporting electrolyte

Analyte	LOD	Linear range	Sensitivity	R^2
Glucose	0.34 μM	1.02 μM to 1 M	I, nA = 0.39 ln[Glu, M] + 1.28	0.9915
Ethanol	0.25 mM	0.75–150 mM	I, nA = 0.19 [EtOH, M] + 0.93	0.9898
Phenol	0.251 nM	0.753 nM to 25 mM	I, nA = 1.69 ln[Ph, M] + 56.47	0.9882

Table 3 Comparison of the results obtained with the proposed ePAD with respect to the declared values for a cider and five beer samples

		Ethanol (v/v%)		Phenols (mM)			Glucose (mM)	
Sample	Type	ePAD	Reported[a]	ePAD	Reported[a]	IBU	ePAD	Reported[a]
OYAH	Cider	6.0 ± 0.9	6.0	1.3 ± 0.5	1.318 ± 0.001	0	50.12 ± 0.02	59.03
Fresh as Helles	Lager	5.4 ± 0.9	5.4	1.9 ± 0.5	1.726 ± 0.001	18	0 ± 1	0
Cherry Wheat	Wheat ale	5.3 ± 0.8	5.3	3 ± 1	2.441 ± 0.001	23	0 ± 1	0
Ghost Rider	Lager	6.1 ± 0.6	6.0	6 ± 2	6.4577 ± 0.0005	55	ND	ND
Palate Wrecker	IPA	9.5 ± 0.6	9.5	12 ± 4	10.058 ± 0.001	100	ND	ND
Bitch Creek	Brown ale	5.9 ± 0.6	6.0	7.7 ± 0.9	6.842 ± 0.003	60	ND	ND

[a] Analyte content declared or detected by spectrophotometry (ESI).

8 g per 750 mL bottle, the ePAD measurement yielded a content of 6.8 g per 750 mL, a difference that was attributed to the selectivity of glucose oxidase towards glucose (and not other carbohydrates).[64] It was also found that the obtained alcohol percentage matched the printed labels with 98–100% accuracy over the concentration range between 5.3 and 9.5% thereby demonstrating the potential practical applicability of the device. Furthermore, we have also observed a direct correlation between the phenol concentration and the bitterness of the selected beers, reported as International Bitterness Units (IBU). This observation further supports the established understanding that the phenols (among other compounds from the hops) are responsible for the bitter taste of beers.

4. Conclusions

The use of a commercially available carbon tape as a simple and effective electrode for electrochemical detection on paper-based microfluidic devices was demonstrated. The tape can be used as either the working or reference electrode. The modification of the μPADs with carbon nanotubes was implemented for the enhanced detection of H_2O_2, the common target of many biosensors. The applicability of the proposed device was demonstrated by measuring glucose, ethanol, and phenols in beers and ciders with good accuracy when compared to the reported concentration on the printed labels.

Conflicts of interest

There are no conflicts to declare.

Acknowledgements

The authors would like to acknowledge partial financial support to this project from Clemson University, the Greenville Health System, Consejo Nacional de Investigaciones Científicas y Técnicas (CONICET) and Facultad de Ciencias Agrarias, Universidad Nacional de Cuyo (Mendoza, Argentina). F. G. also acknowledges the support from a Fulbright Scholarship.

References

1 T. Akyazi, L. Basabe-Desmonts and F. Benito-Lopez, *Anal. Chim. Acta*, 2018, **1001**, 1–17.
2 A. W. Martinez, S. T. Phillips, G. M. Whitesides and E. Carrilho, *Anal. Chem.*, 2010, **82**, 3–10.
3 A. W. Martinez, S. T. Phillips, M. J. Butte and G. M. Whitesides, *Angew. Chem., Int. Ed.*, 2007, **46**, 1318–1320.
4 T. Arfin and S. N. Rangari, *Anal. Methods*, 2018, **10**, 347–358.
5 J. Kang, Y. Zhang, X. Li, C. Dong, H. Liu, L. Miao, P. Low, Z. Gao, N. Hosmane and A. Wu, *Anal. Methods*, 2018, **10**, 417–421.
6 G. Bulbul, H. Eskandarloo and A. Abbaspourrad, *Anal. Methods*, 2018, **10**, 275–280.
7 M. Urdea, L. A. Penny, S. S. Olmsted, M. Y. Giovanni, P. Kaspar, A. Shepherd, P. Wilson, C. A. Dahl, S. Buchsbaum, G. Moeller and D. C. Hay Burgess, *Nature*, 2006, **444**, 73–79.
8 S. Cinti, L. Fiore, R. Massoud, C. Cortese, D. Moscone, G. Palleschi and F. Arduini, *Talanta*, 2018, **179**, 186–192.
9 A. K. Yetisen, M. S. Akram and C. R. Lowe, *Lab Chip*, 2013, **13**, 2210–2251.
10 J. A. Adkins and C. S. Henry, *Anal. Chim. Acta*, 2015, **891**, 247–254.
11 J. Mettakoonpitak, K. Boehle, S. Nantaphol, P. Teengam, J. A. Adkins, M. Srisa-Art and C. S. Henry, *Electroanalysis*, 2016, **28**, 1420–1436.

12 W. Dungchai, O. Chailapakul and C. S. Henry, *Anal. Chem.*, 2009, **81**, 5821–5826.
13 J. Adkins, K. Boehle and C. Henry, *Electrophoresis*, 2015, **36**, 1811–1824.
14 D. M. Cate, J. A. Adkins, J. Mettakoonpitak and C. S. Henry, *Anal. Chem.*, 2015, **87**, 19–41.
15 E. W. Nery and L. T. Kubota, *Anal. Bioanal. Chem.*, 2013, **405**, 7573–7595.
16 P. Sjöberg, A. Määttänen, U. Vanamo, M. Novell, P. Ihalainen, F. J. Andrade, J. Bobacka and J. Peltonen, *Sens. Actuators, B*, 2016, **224**, 325–332.
17 J. M. Petroni, B. G. Lucca, L. C. da Silva Júnior, D. C. Barbosa Alves and V. Souza Ferreira, *Electroanalysis*, 2017, **29**, 2628–2637.
18 E. B. Secor and M. C. Hersam, Graphene Inks for Printed Electronics, https://www.sigmaaldrich.com/technical-documents/articles/technology-spotlights/graphene-inks-for-printed-electronics.html, accessed 30 April 2018.
19 C. Hu, X. Bai, Y. Wang, W. Jin, X. Zhang and S. Hu, *Anal. Chem.*, 2012, **84**, 3745–3750.
20 E. Gabriel, W. Coltro and C. Garcia, *Electrophoresis*, 2014, **35**, 2325–2332.
21 E. Evans, E. Gabriel, T. Benavidez, W. Coltro and C. Garcia, *Analyst*, 2014, **139**, 5560–5567.
22 Z. Nie, C. Nijhuis, J. Gong, X. Chen, A. Kumachev, A. Martinez, M. Narovlyansky and G. Whitesides, *Lab Chip*, 2010, **10**, 477–483.
23 A. F. Stalder, T. Melchior, M. Müller, D. Sage, T. Blu and M. Unser, *Colloids Surf., A*, 2010, **364**, 72–81.
24 L. McCann, T. E. Benavidez, S. Holtsclaw and C. D. Garcia, *Analyst*, 2017, 3899–3905.
25 K. Imoto, K. Takahashi, T. Yamaguchi, T. Komura, J. Nakamura and K. Murata, *Sol. Energy Mater. Sol. Cells*, 2003, **79**, 459–469.
26 J. Giuliani, T. Benavidez, G. Duran, E. Vinogradova, A. Rios and C. Garcia, *J. Electroanal. Chem.*, 2016, **765**, 8–15.
27 T. Benavidez and C. Garcia, *Electrophoresis*, 2013, **34**, 1998–2006.
28 S. Alharthi, T. Benavidez and C. Garcia, *Langmuir*, 2013, **29**, 3320–3327.
29 K. Scida, P. Stege, G. Haby, G. Messina and C. Garcia, *Anal. Chim. Acta*, 2011, **691**, 6–17.
30 C.-S. Lee, S. H. Yu and T. H. Kim, *Nanomaterials*, 2018, **8**, 17–30.
31 M. Faraji and M. Mohseni, *Ionics*, 2018, DOI: 10.1007/s11581-017-2416-z.
32 T. Sarkar, H. B. Bohidar and P. R. Solanki, *Int. J. Biol. Macromol.*, 2018, **109**, 687–697.
33 Y. Wang, D. Alsmeyer and R. McCreery, *Chem. Mater.*, 1990, **2**, 557–563.
34 R. Saito, M. Hofmann, G. Dresselhaus, A. Jorio and M. Dresselhaus, *Adv. Phys.*, 2011, **60**, 413–550.
35 T. E. Benavidez, R. Martinez-Duarte and C. D. Garcia, *Anal. Methods*, 2016, **8**, 4163–4176.
36 P. Chen and R. L. McCreery, *Anal. Chem.*, 1996, **68**, 3958–3965.
37 P. Diakowski, Y. Xiao, M. Petryk and H. Kraatz, *Anal. Chem.*, 2010, **82**, 3191–3197.
38 S. Basuray, S. Senapati, A. Aijian, A. Mahon and H. Chang, *ACS Nano*, 2009, **3**, 1823–1830.
39 M. Cabral, J. Barrios, E. Kataoka, S. Machado, E. Carrilho, C. Garcia and A. Ayon, *Colloids Surf., B*, 2013, **103**, 624–629.
40 O. Filipe and C. Brett, *Electroanalysis*, 2004, **16**, 994–1001.
41 J. M. Goran, E. N. H. Phan, C. A. Favela and K. J. Stevenson, *Anal. Chem.*, 2015, **87**, 5989–5996.
42 S. A. Bhakta, E. Evans, T. E. Benavidez and C. D. Garcia, *Anal. Chim. Acta*, 2015, **872**, 7–25.
43 M. R. Nejadnik, F. L. Deepak and C. D. Garcia, *Electroanalysis*, 2011, **23**, 1462–1469.
44 J. L. Felhofer, J. D. Caranto and C. D. Garcia, *Langmuir*, 2010, **26**, 17178–17183.
45 M. Rubianes and G. Rivas, *Electroanalysis*, 2005, **17**, 73–78.
46 F. Ricci and G. Palleschi, *Biosens. Bioelectron.*, 2005, **21**, 389–407.
47 @BrewersAssoc, National Beer Sales & Production Data, https://www.brewersassociation.org/statistics/national-beer-sales-production-data/.
48 G. Fox, *J. Inst. Brew.*, 2016, **122**, 437–445.
49 A. Olaniran, L. Hiralal, M. Mokoena and B. Pillay, *J. Inst. Brew.*, 2017, **123**, 13–23.
50 T. Branyik, D. Silva, M. Baszczynski, R. Lehnert and J. Silva, *J. Food Eng.*, 2012, **108**, 493–506.
51 I. Duarte, A. Barros, P. Belton, R. Righelato, M. Spraul, E. Humpfer and A. Gil, *J. Agric. Food Chem.*, 2002, **50**, 2475–2481.
52 S. Cortacero-Ramirez, M. de Castro, A. Segura-Carretero, C. Cruces-Blanco and A. Fernandez-Gutierrez, *Trends Anal. Chem.*, 2003, **22**, 440–455.
53 E. Sikorska, A. Glisuzynska-Swiglo, M. Insinska-Rak, I. Khmelinskii, D. De Keukeleire and M. Sikorski, *Anal. Chim. Acta*, 2008, **613**, 207–217.
54 M. Rossi, D. Vidal and C. do Lago, *Food Chem.*, 2012, **133**, 352–357.
55 D. Daniel, V. dos Santos, D. Vidal and C. do Lago, *J. Chromatogr. A*, 2015, **1416**, 121–128.
56 L. Nogueira, F. Silva, I. Ferreira and L. Trugo, *J. Chromatogr. A*, 2005, **1065**, 207–210.
57 L. Wang, Y. He, F. Liu and X. Ying, *J. Infrared, Millimeter, Terahertz Waves*, 2008, **27**, 51–55.
58 M. Dvorakova, P. Hulin, M. Karabin and P. Dostalek, *Czech J. Food Sci.*, 2007, **25**, 182–188.
59 H. Yamamoto, C. Nagano, F. Takeuchi, J. Shibata, M. Tagashira and Y. Ohtake, *J. Chem. Eng. Jpn.*, 2006, **39**, 956–962.
60 P. Lehtonen and R. Hurme, *J. Inst. Brew.*, 1994, **100**, 343–346.
61 W. Kirby and R. Wheeler, *J. Inst. Brew.*, 1980, **86**, 15–17.
62 Z. Nie, F. Deiss, X. Liu, O. Akbulut and G. Whitesides, *Lab Chip*, 2010, **10**, 3163–3169.
63 N. Dossi, R. Toniolo, F. Terzi, E. Piccin and G. Bontempelli, *Electrophoresis*, 2015, **36**, 1830–1836.
64 S. Bankar, M. Bule, R. Singhal and L. Ananthanarayan, *Biotechnol. Adv.*, 2009, **27**, 489–501.